CORA Cork Open Research Archive
Cartlann Taighde Oscailte Chorcaí

Title	Novel high frequency electrical characterization technique for magnetic passive devices
Authors	Fernandez, Cristina;Pavlović, Zoran;Kulkarni, Santosh;McCloskey, Paul;Ó Mathúna, S. Cian
Publication date	2018-01-28
Original Citation	Fernandez, C., Pavlovic, Z., Kulkarni, S., McCloskey, P. and Mathúna, C. Ó. (2018) 'Novel High Frequency Electrical Characterization technique for Magnetic Passive Devices', IEEE Journal of Emerging and Selected Topics in Power Electronics, 6(2), pp. 621-628. doi: 10.1109/JESTPE.2018.2798919
Type of publication	Article (peer-reviewed)
Link to publisher's version	10.1109/JESTPE.2018.2798919
Rights	© 2018 IEEE. Personal use of this material is permitted. Permission from IEEE must be obtained for all other uses, in any current or future media, including reprinting/republishing this material for advertising or promotional purposes, creating new collective works, for resale or redistribution to servers or lists, or reuse of any copyrighted component of this work in other works.
Download date	2024-10-12 04:51:47
Item downloaded from	https://hdl.handle.net/10468/5552

UCC
University College Cork, Ireland
Coláiste na hOllscoile Corcaigh

This article has been accepted for publication in a future issue of this journal, but has not been fully edited. Content may change prior to final publication. Citation information: DOI 10.1109/JESTPE.2018.2798919, IEEE Journal of Emerging and Selected Topics in Power Electronics

JESTPE-2017-04-0322.R1

Novel High Frequency Electrical Characterization technique for Magnetic Passive Devices

Cristina Fernandez, *Member, IEEE*, Zoran Pavlovic, *Member, IEEE*, Santosh Kulkarni, *Member, IEEE*, Paul McCloskey, *Member, IEEE* and Cian Ó Mathúna, *Fellow, IEEE*

***Abstract*— Integrated magnetic components are key elements of the Power Supply on Chip modules. Due to the application requirements, these magnetic devices work at very high frequency and have low inductances. Conventional small-signal tests do not provide all the required information about the magnetic device. Hence, it is important to develop new set-ups to apply large signals to accurately measure the performance of devices under realistic operating conditions, including non-linear core effects. The proposed experimental set-up is suitable to measure the device impedance under different large-signal test conditions, similar to those in the actual converter, since the excitation current can be configured through every winding: ac current up to 0.5 A at frequencies up to 120 MHz and dc bias current up to 2 A through one or both windings. Voltage and current are measured using commercial instrumentation. Due to the characteristics of the probes and the high frequency of the test, the attenuation and delay due to the probes and the experimental set-up have to be taken into account when processing the voltage and current waveforms to calculate the impedances. The compensation test to calculate this attenuation and delay is described. Finally, the proposed set-up is validated by measuring a two-phase coupled inductors micro-fabricated on silicon.**

***Index Terms*— dc-dc converters, impedance measurement, integrated magnetics, thin-film inductors, large signal testing**

I. Introduction

THE ever-increasing drive towards miniaturization, increased functionality and higher efficiency of electronic devices has highlighted the challenge of delivering power efficiently to these devices. Granular Voltage Regulation (VR) is increasingly seen as solution to address the power requirements of multi-functional electronic device. These granular VRs can be placed at the point-of-load minimizing the efficiency losses due to parasitic interconnects. This is typically achieved as a Power System in Package (PwrSiP) or Power System on Chip (PwrSoC) where the VR is either packaged or monolithically built with load [1]. Apart from improved parasitic losses, this approach also provides benefits of improved dynamic response from the VR based on the requirements of the load. Additionally, granular VR's use multi-phase topologies where the concept of phase shedding also provides improved light load efficiencies as compared to single phase topologies [2-6].

A buck type dc-dc converter is the most commonly employed topology for Integrated VR (IVR), since it offers higher efficiency compared to linear and hybrid regulators and performs step down function as required by the applications. Typically, a buck converter circuit employs inductors to store the electrical energy temporarily. These magnetic devices use a soft magnetic material core to store the energy efficiently. The use of soft magnetic cores significantly increases the energy density of the inductor in comparison to an air-core device without the soft magnetic core [6-9]. Traditional inductor structures use ferrite magnetic cores owing to ferrite's low cost and ultra-low power loss density. Advanced power switching circuits employing faster switches and drivers, reduce the energy storage requirement in these devices, enabling the use of alternate thin film soft magnetic materials as cores. A key advantage of thin film materials is their higher saturation flux density which enables devices with smaller footprint and volume, in comparison to lower saturation density ferrite based devices. Additionally, thin film alloys can be processed on silicon substrates with MEMS based fabrication techniques [7], allowing further integration of these passive devices with other active components fabricated on silicon. Considerable effort has been made to design and construct suitable magnetic core for inductors to be used in IVR applications, [5-10]. However, most soft magnetic thin films have higher losses in comparison to ferrites, particularly in relation to eddy current losses, as they are much more conductive. Moreover, although the higher

This work was supported in part by the EU PowerSwipe project under Grant 318529, the Science Foundation Ireland (Investigators programme 15/IA/3180), and the Spanish Ministry of Economy and Competitiveness and FEDER funds (projects DPI2014-53685-C2-1-R and DPI2017-88062-R).

C. Fernandez is with the Power Electronics System Group GSEP, Universidad Carlos III de Madrid, Spain (e-mail: cfernand@ing.uc3m.es).

Z. Pavlovic, S. Kulkarni P. McCloskey and C. O'Mathuna are with the ´ Microsystems Centre, Tyndall National Institute, Cork T12 R5CP, Ireland (e-mail: zoran.pavlovic@tyndall.ie; santosh.kulkarni@tyndall.ie; paul.mccloskey@tyndall.ie; cian.omathuna@tyndall.ie). C. O'Mathuna is also with the Department of Electrical and Electronics Engineering, University College Cork, Cork, Ireland.

2168-6777 (c) 2018 IEEE. Personal use is permitted, but republication/redistribution requires IEEE permission. See http://www.ieee.org/publications_standards/publications/rights/index.html for more information.

This article has been accepted for publication in a future issue of this journal, but has not been fully edited. Content may change prior to final publication. Citation information: DOI 10.1109/JESTPE.2018.2798919, IEEE Journal of Emerging and Selected Topics in Power Electronics

permeability of thin film materials enables miniaturization, a disadvantage of higher permeability is that when such materials are used in single phase inductors, the shorter magnetic path length for smaller devices limit the current handling capability of the device. This challenge is addressed through the use of inductors with negatively coupled phases, in which opposing flux is induced in the core resulting in flux cancellation thus enabling the cores to handle higher currents. Additionally, the negatively coupled phases reduce the output ripple, through reduced summation of currents in different phases and also the energy is stored in the leakage inductance of the device enabling faster transient response to the load.

As explained earlier, the use of soft magnetic thin films is enabled by faster switching circuits and increasingly, researchers have focused on developing new magnetic thin films alloys and device constructions, capable of operating at very high frequencies beyond 100 MHz. Core losses are highly non-linear with both frequency and B-field, reinforcing the importance of empirical characterization, not modeling, as the best route to design the component. This accentuates the challenge of characterizing these materials and devices at high frequency. Characterization at high frequencies using network analyzers is widely used, but only a small signal current is applied, and hence this characterization only provides information concerning copper and core eddy current losses. A large signal characterization set-up is required to accurately measure the loss performance of coupled inductor device before a full VR test [5].

The large signal characterization conditions are typically selected to match those of the actual converter, so the device impedance measurement gives the total core loss including eddy current, hysteresis and excess eddy current losses. The key issues to be addressed in a large-signal measurement system are the generation of an adequate excitation signal as well as a high-precision method to measure the equivalent impedance. There have been a significant number of reports on large signal characterization of discrete passive devices [11-13]. However, work on integrated thin film devices has been challenging due to the need for high frequency characterization. This work presents the large signal tests performed to characterize a device up to 120 MHz. The paper also discusses the challenges in terms of acquiring accurate voltage and current data at these frequencies along with the challenge of compensation for the lag in the probes.

II. Large Signal Measurement Set-Up at High Frequency

A. *Proposed large signal set-up*

A typical approach to large signal characterization of an on-silicon coupled inductor is through applying the appropriate excitation either in one or two phases and measuring the voltage and current to calculate its impedance. A key challenge is the accurate extraction of the voltage and current waveforms at very high frequencies.

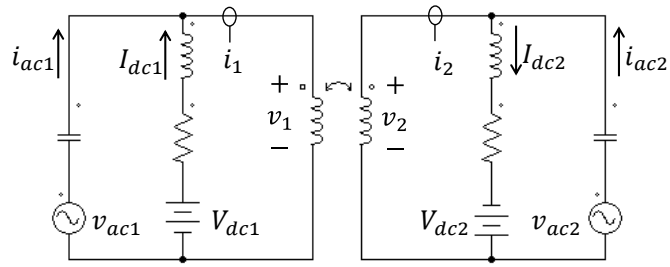

Fig. 1 Schematic of the large signal testing circuit

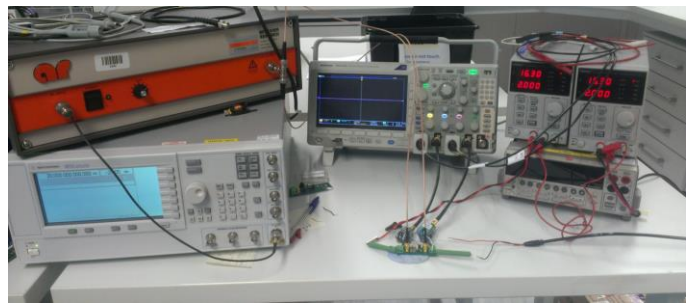

Fig. 2 Large signal set-up

The proposed experimental set-up, whose schematic is represented in Fig. 1, has been designed in order to: 1) set the conditions as similar as possible to those that the device would have on the actual converter, producing both ac and dc currents through one or both windings; 2) improve the accuracy of the measurements at very high frequencies using commercial probes to sense voltage and current.

Measuring the voltage and current waveforms (v_1, i_1, v_2, i_2) and depending on the applied voltages ($v_{ac1}, V_{dc1}, V_{dc2}, v_{ac2}$), indicated in Fig. 1, the self-impedance or the mutual impedance can be calculated under different working conditions. Thus, the self-impedance of the primary winding Z_{11} is calculated by measuring v_1 and i_1, while the core-impedance Z_{12} is calculated by measuring v_2 and i_1. The inductive component is calculated directly as the imaginary part of the impedance while the resistive component is the real part of the impedance.

Fig. 2 provides a picture of the set-up. The excitation signals for each winding, shown in the schematic in Fig. 1, are generated by two different branches connected in parallel:

- Generation of the ac signal (v_{ac1} and v_{ac2}): a RF-amplifier, controlled by a signal generator, injects the ac current to the PCB circuit through an SMA connector. The RF Amplifier is series-connected to a dc blocking capacitor.
- Generation of the dc current (V_{dc1} and V_{dc2}): an independent dc source is series-connected with an inductance to block the ac current and a power resistor to limit the total current.

2168-6777 (c) 2018 IEEE. Personal use is permitted, but republication/redistribution requires IEEE permission. See http://www.ieee.org/publications_standards/publications/rights/index.html for more information.

This article has been accepted for publication in a future issue of this journal, but has not been fully edited. Content may change prior to final publication. Citation information: DOI 10.1109/JESTPE.2018.2798919, IEEE Journal of Emerging and Selected Topics in Power Electronics

TABLE I
EQUIPMENT AND COMPONENTS USED IN THE LARGE SIGNAL SET-UP

RF-amplifier	Amplifier Research 25A250A
Signal generator	Agilent E8257D
dc blocking capacitor	2 SMD 100 nF 25 V
Independent DC sources	DENMA T2-10480
Series inductor	SMD 1210 2.2 µH from Kemet, model L1210R2R2MDWIT
Series power resistor	10 Ω
Data acquisition	Tektronix MDO3104
Voltage probe	Tektronix TAP1500
Current probe	Pearson Current Monitor model 2877

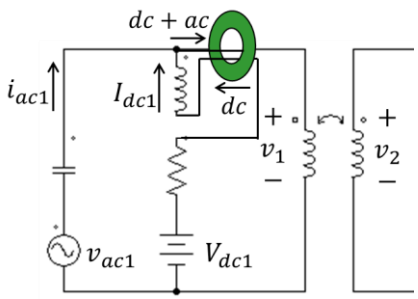

Fig. 3 Compensation of the dc current through the current monitor to avoid saturation

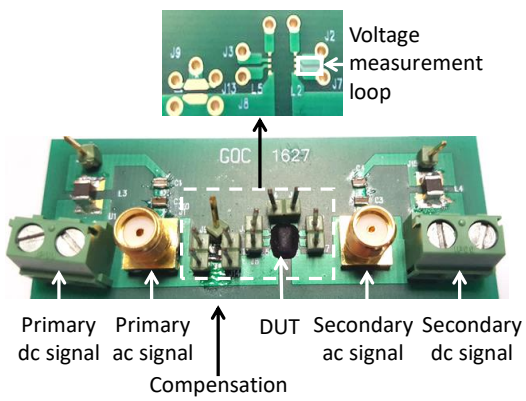

Fig. 4 Large signal testing circuit

The designed set-up, summarized in Table I, allows applying dc bias current up to 2 A and ac current through both windings up to 120 MHz. The data acquisition is done using a mixed domain oscilloscope, while voltage and current are measured using commercial probes:

- Voltage probes: the selected voltage probes are the Tektronix TAP1500, with an impedance of approximately 1 pF. At high frequency, the impedance of the probes could introduce an additional path for the current and thus it is critical to use high impedance probes for improved accuracy. This issue is reported in [14, 15].
- Current probes: the Pearson Current Monitor model 2877 is selected for the current measurements due to its bandwidth (200 MHz) and low delay [16, 17], in contrast to the use of resistors, as is often reported in the literature [12, 13, 18, 19]. The measured current has no harmonics to worry about non-linearity of the current probe. However, it is only suitable for ac current and saturates at moderate values of dc bias. To avoid saturation, the dc current is compensated through the current monitor. The schematic in Fig. 3 shows this compensation (primary side). Since the dc choke self-resonance is around 190 MHz (series inductance in Table I), no ac current is expected in the dc branch that could spoil the current measurement.

There are different sources of errors that could affect the accuracy of the measurements [11]. Due to the proposed methodology, the main sources of errors in this approach are:

- Circuit parasitics: the PCB has been designed to minimize the impact of the circuit parasitics. The designed PCB is shown in Fig. 4, as well as the detail of the connections of the device under test (DUT). The voltage measurements in the terminals of the magnetic device have been taken by using a 4-terminal Kelvin connection, being the driven current traces separated to the voltage measurement traces. Ac mutual resistance should not be a problem because current in the voltage measurement loop is extremely small. Mutual inductance could induce voltage in the measurement loop, but to minimize the effect of the parasitics in the voltage measurement, the voltage probes are connected as close as possible to the device itself, that is, the shaded area in Fig. 4 is made as small as possible. Thus, error due to layout parasitics is considered negligible in this work.
- Probes: since the impedance is measured directly from the voltage and current waveforms, the probes themselves become the main potential source of error:
  - Error in amplitude. The current monitors exhibit amplitude response as a function of the frequency and so the current waveform can be attenuated. This attenuation should be measured and taken into account during the post-processing of the waveforms.
  - Delay between the signals. Voltage and current probes have their own characteristic propagation delay, so the current and voltage waveforms measured by the scope can be time-skewed relative to each other. This means that the data pairs are not time coincident, and thus it is mandatory to provide a way to correct the time-skew during the post-processing of the waveforms [20, 21].

According to the identified sources of error, a compensation test is required to minimize the impact of the probes in the accuracy of the measurement. Therefore, the first step is to determine the attenuation due to the measurement system, as well as the time delay between channels.

B. *Compensation test*

The compensation test is performed measuring the voltage

2168-6777 (c) 2018 IEEE. Personal use is permitted, but republication/redistribution requires IEEE permission. See http://www.ieee.org/publications_standards/publications/rights/index.html for more information.

This article has been accepted for publication in a future issue of this journal, but has not been fully edited. Content may change prior to final publication. Citation information: DOI 10.1109/JESTPE.2018.2798919, IEEE Journal of Emerging and Selected Topics in Power Electronics

across and the current through an impedance Z known at the frequency of the test (Fig. 5). In this case a high-Q SMD with a 220 nF capacitance has been chosen for the compensation test (compensation block in Fig. 4). The capacitor CC0402JRNPO9BN221 with Class 1 NP0 dielectric presents a negligible variation of capacitance and equivalent series resistance with frequency. It was tested in small-signal with an E4990 Impedance Analyzer and Qc=tan(89.3º)=81 at 100 MHz. Based on these data, the capacitor at 100 MHz is very close to an ideal one. In addition, its impedance decreases with frequency causing the current to increase, which has the benefit of increasing the signal to noise ratio.

The first harmonics of the measured voltage and current v_1 and i_1 are calculated, being $\underline{V_1}$ and $\underline{I_1}$. Then voltage and current are compared to the theoretical ones to calculate the $Attenuation$ and $Phaseshift$ introduced by the probes and the measurement system, calculated by means of (1) and (2). Therefore, to accurately calculate any impedance using the proposed set-up, it is required to post-process the measured voltage and current waveforms to compensate the attenuation and to de-skew using the calculated $Attenuation$ and $Phaseshift$ at every frequency.

$$Attenuation = \frac{|\underline{I_1}||\underline{Z}|}{|\underline{V_1}|} \quad (1)$$

$$Phaseshift = \angle\underline{V_1} - \angle\underline{I_1} - \angle\underline{Z} \quad (2)$$

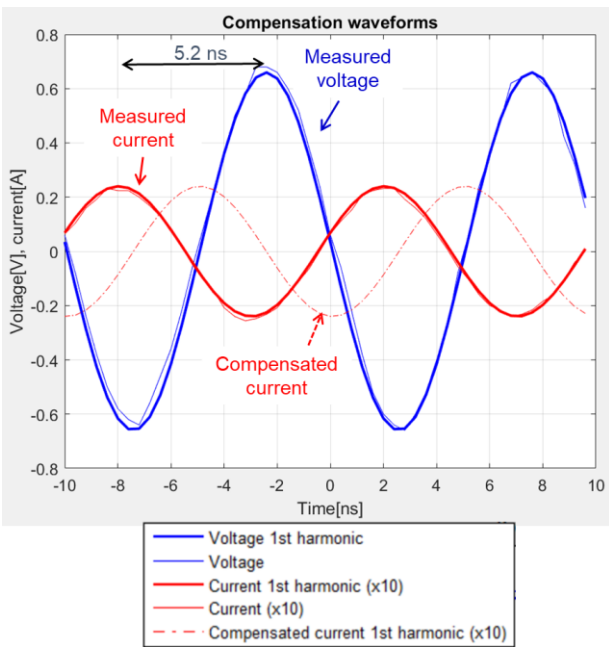

Fig. 6 Measured voltage and current waveforms in a compensation test at 100 MHz

TABLE II
CHARACTERISTICS OF THE COUPLED INDUCTORS UNDER TEST

Inductance	47 nH
Coupling coefficient	0.4
Core thickness	1.6 µm
Core length	1.78 mm
Copper width	50.62 µm
Copper thickness	15 µm
DCR	0.3425 Ω
Device footprint	2 mm2

The importance of the compensation test can be understood by observing the waveforms in Fig. 6, measured at 100 MHz. The waveforms represented with continuous lines correspond to the signals measured in the compensation test. It can be observed that the phase shift between the measured voltage and current is completely different to what would be expected in a high-Q capacitor. The dotted line represents the current post-processed including the calculated attenuation and phase shift. The delay observed is quite consistent with what would be expected based on the hardware used. According to the data sheets, which do not include tolerances, the delay of the voltage probe is 5.3 ns and the delay of the current monitor at 100 MHz approximately 0.2 ns (6 deg). Theoretically, voltage would be shifted 7.6 ns with respect to the current without considering the propagation time of the cable for the current measurement, which will reduce this value. The measured time shift between signals is 5.2 ns (Fig. 6).

III. VALIDATION TEST USING ON-SILICON COUPLED INDUCTOR DEVICES

A. Description of the magnetic device

To validate the proposed test methodology a two-phase coupled inductor micro-fabricated on silicon is characterized. The specifications of the magnetic device are given in Table II, while a picture of the fabricated device structure is shown in Fig. 7.a. The device is formed by two coupled equal coils with self-inductance equal to 47 nH and a coupling factor of less than 0.4. The magnetic core is made of polycrystalline $Ni_{45}Fe_{55}$ and the windings only share the central leg (Fig. 7.b), which is the reason of the low magnetic coupling. The design, fabrication and small signal characterization of this device is reported in previous publications [7, 10], as well as a first large signal characterization for frequencies less than 15 MHz [22]. Also some preliminary results of the measurements using the proposed set-up were provided in [14, 15].

The magnetic device was first characterized performing a small-signal test using a 2-port Vector Network Analyzer E8361A with a GS probe. The results are depicted in Fig. 8. The four plots represent the self-inductance of primary (L_{11}) and secondary (L_{22}) of two different samples (1 and 2). Any variations in the measured data between samples are assumed to be by deviations in the manufacturing process.

An additional small-signal test, performed at 10 MHz and varying the bias dc current through the primary winding, is depicted in Fig. 9. The saturation current level, defined as the current where a 20% drop in the inductance value occurs, is approximately 650 mA.

2168-6777 (c) 2018 IEEE. Personal use is permitted, but republication/redistribution requires IEEE permission. See http://www.ieee.org/publications_standards/publications/rights/index.html for more information.

This article has been accepted for publication in a future issue of this journal, but has not been fully edited. Content may change prior to final publication. Citation information: DOI 10.1109/JESTPE.2018.2798919, IEEE Journal of Emerging and Selected Topics in Power Electronics

a) Picture of the fabricated device

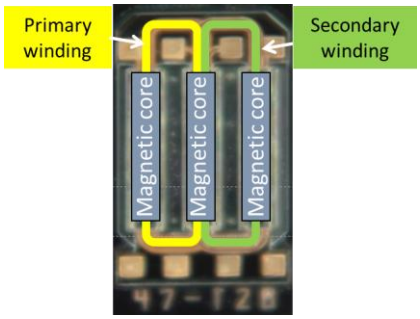

b) Elements of the magnetic device

Fig. 7 Micro-fabricated two phase coupled inductor

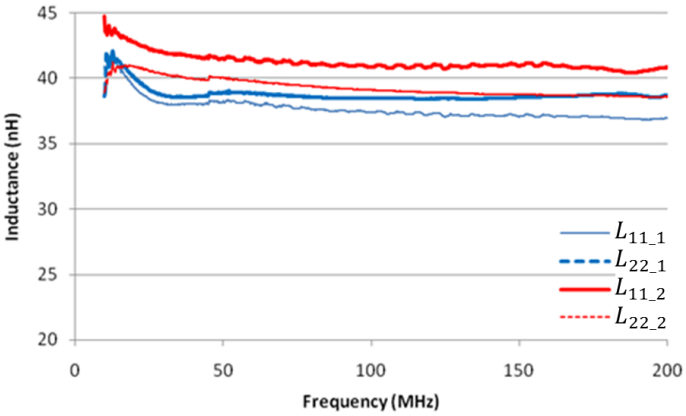

Fig. 8 Small-signal measurements of the self-inductance vs. frequency

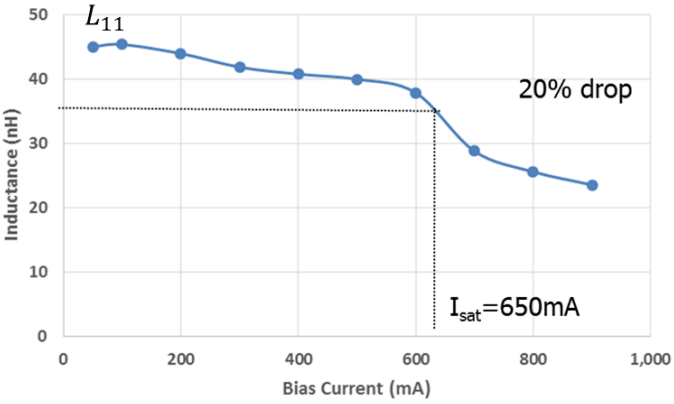

Fig. 9 Small-signal measurements of the primary self-inductance varying the bias dc current through the primary winding

B. *Large Signal Coupled Inductor Measurements & Discussion*

The proposed large signal set-up was used to perform a frequency sweep in similar conditions to the mentioned small-signal test, producing only ac current through the primary winding from 20 MHz to 100 MHz but with a higher amplitude, equal to 30 mA. As shown in Fig. 10, the inductance is not very sensitive to frequency variation. In contrast the measured core resistance plotted in Fig. 11 shows a strong dependence on frequency.

The measurements obtained with the proposed set-up (Fig. 10) are consistent with the inductance measured with the impedance analyzer, plotted in Fig. 8. The inductance measured with the large-signal set-up is higher because of the wire bonding required to connect the magnetic device to the pads on the PCB. In this case, the inductance of the wire bonding is estimated to be 4 nH approximately.

Mutual resistance R_{12} includes magnetic core loss in the central core and mutual winding resistance. From a 2D FEA simulation of the device at 100 MHz with a loss-less core, the mutual winding resistance is the range of few milliohms per mm length of the winding, which is few orders of magnitude smaller than the total measured R12 (Fig. 11). Therefore, the measured mutual resistance can be considered entirely as a magnetic material core loss contribution.

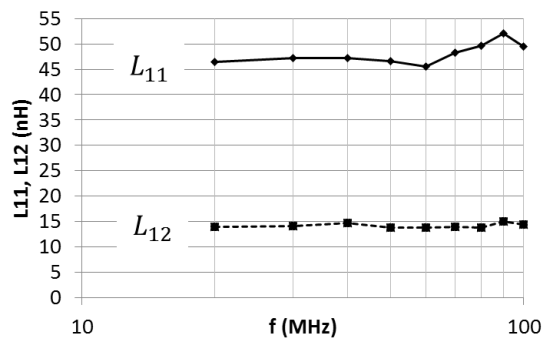

Fig. 10 Self and mutual inductance of the coupled inductor (30 mA ac signal from primary side, no dc)

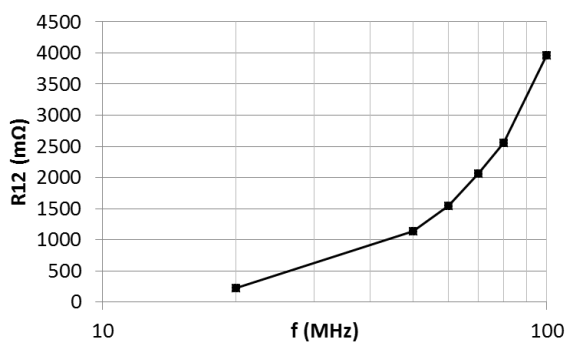

Fig. 11 Core resistance of the coupled inductor (30 mA ac signal from primary side, no dc)

Further large signal tests were carried out, with both ac and

2168-6777 (c) 2018 IEEE. Personal use is permitted, but republication/redistribution requires IEEE permission. See http://www.ieee.org/publications_standards/publications/rights/index.html for more information.

This article has been accepted for publication in a future issue of this journal, but has not been fully edited. Content may change prior to final publication. Citation information: DOI 10.1109/JESTPE.2018.2798919, IEEE Journal of Emerging and Selected Topics in Power Electronics

dc current applied, varying the dc bias current from 0 to 1.5 A but with a higher ac amplitude, equal to 100 mA:

- "Single dc" test: dc and ac currents are produced only through the primary winding. This test is done in a similar way to the small-signal test reported in Fig. 9, but with a higher ac amplitude.
- "Dual dc" test: ac current is produced through the primary winding and dc current through both primary and secondary windings. This test reproduces more accurately the actual operating conditions of the magnetic device in the dc-dc converter.

The measured self and mutual inductances at 100 MHz are shown in Fig. 12.a. The plot compares both tests, which provide very different results due to the behavior of the magnetic core. In the single dc test, both self and mutual inductances decrease with applied dc bias current. This is consistent with theory: as the core is excited with a field close to saturation field, the relative permeability becomes lower, resulting in a lower inductance. Notice that using the proposed approach, inductance is calculated on a period by means of the first harmonic current and voltage. This apparent inductance does not account for all the non-linear effects that occur in large signal when the device is saturated, but provides a good idea of when the saturation is reached. For this single dc test, the saturation current level is approximately 600 mA, lower than the one reported in the small-signal test shown in Fig. 9.

The reason is the higher ac current produced through the winding in this test. The calculated magnetic coupling for the single dc test, depicted in Fig. 12.b, decreases with applied dc bias current.

On the other hand, the mutual inductance measured from the dual dc test is very insensitive to the bias current level, as shown in Fig. 12.a. The reason is that dc currents flow in opposite directions through primary and secondary windings, cancelling its net effect in the central leg of the magnetic core, which does not saturate. Eventually the self-inductance decreases with applied dc bias current, but the saturation current level (1.4 A) is much higher than applying the single dc test. This is because in the dual dc test only the outer leg of the primary winding is saturating. Looking at the calculated magnetic coupling in Fig. 12.b, coupling increases with applied dual dc current, since the magnetizing inductance remains constant while the self-inductance decreases.

Further large signal tests were carried out with dc currents applied through both windings and ac current only through the primary winding (dual dc). These tests were done at three different frequencies: 80 MHz, 100 MHz and 120 MHz. The comparison of the self and mutual inductances is done in Fig. 13, showing trends like the ones reported from the previous tests: the mutual inductance is not sensitive to the dc current level while the self-inductance decreases.

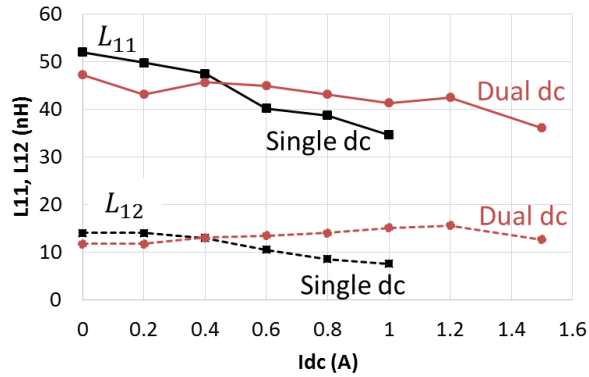

a) Self-inductance L11 and mutual inductance L12

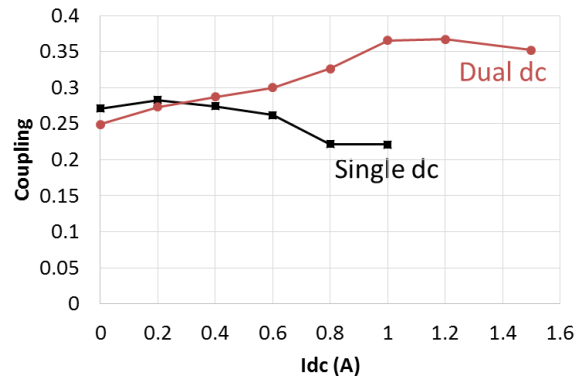

b) Magnetic coupling

Fig. 12 Measurements from the single dc and dual dc tests performed at 100 MHz with ac amplitude equal to 100 mA

The resistances measured from these tests are plotted in Fig. 14. As expected, resistance increases with frequency. Core resistance remains approximately constant despite dc bias level for the same reason that the mutual inductance: because the dc currents through both windings are cancelling in the central leg and so its effect is negligible. On the other hand, self-resistance drops due to the saturation of the outer leg of the core.

From the measured voltage and current is possible to calculate the BH curve at the different working points, as shown for two tests in Fig. 15. This plot is very interesting for a better understanding of the variations of the permeability and the coercivity.

One of the most relevant conclusions from these tests is the importance of the large-signal testing: the excitation of the magnetic device inside the dc-dc converter is more similar to the dual dc test than the single dc or the small signal test. Considering the compared measurements, the behavior of the coupled inductor could not be predicted from the conventional small-signal test results plotted in Fig. 8 and Fig. 9, since the core saturation effects are different when dc current flows through both windings, as reported in Fig. 13.

2168-6777 (c) 2018 IEEE. Personal use is permitted, but republication/redistribution requires IEEE permission. See http://www.ieee.org/publications_standards/publications/rights/index.html for more information.

This article has been accepted for publication in a future issue of this journal, but has not been fully edited. Content may change prior to final publication. Citation information: DOI 10.1109/JESTPE.2018.2798919, IEEE Journal of Emerging and Selected Topics in Power Electronics

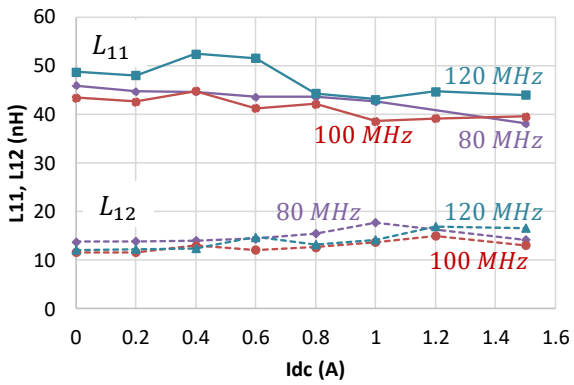

Fig. 13 Measurements from dual dc tests performed at different frequencies, with ac amplitude equal to 100 mA

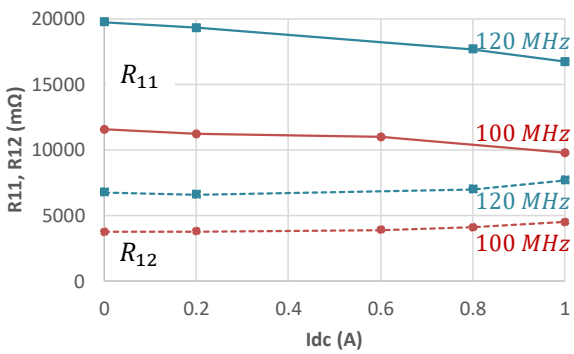

Fig. 14 Measured self and core resistances from dual dc tests performed at different frequencies, with ac amplitude equal to 100 mA

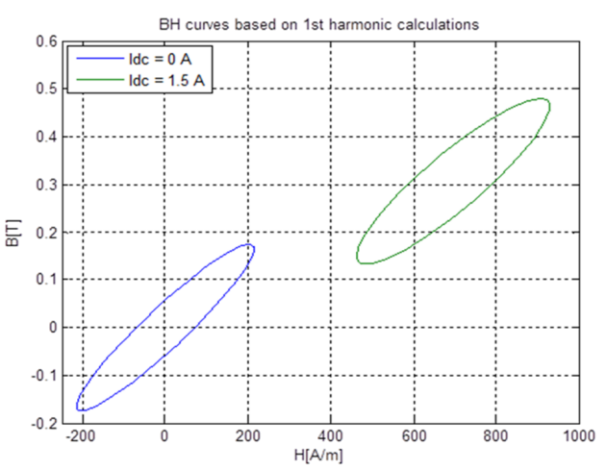

Fig. 15 B-H loops calculated from the dual dc tests at 100 MHz

IV. Conclusion

This work presents the experimental set-up and the methodology used to test coupled inductors at very high frequency (up to 120 MHz). This set-up allows measuring the performance of the magnetic device under realistic operating conditions close to those in a dc-dc converter, that is, producing ac and dc current through one or two windings.

The measurements are performed using commercial instrumentation. Due to the characteristics of the voltage and current probes and the high frequency of the test, the effect of the probes has to be compensated by performing a compensation test to calculate the attenuation and the delay. These values have to be taken into account when processing the voltage and current waveforms to calculate the impedances.

The proposed set-up has been validated by testing two-phase coupled inductors micro-fabricated on silicon with a self-inductance equal to 47 nH. Measurements have been presented with up to a 1.5 A bias current and up to 120 MHz. There are significant differences in the measurements when dc current is produced through one or two windings due to the non-linear effects of the magnetic core. These results highlight the importance of the large-signal test to accurately predict the behavior of the magnetic device in the actual converter, to calculate in advance the current ripple and efficiency of the circuit.

References

[1] C. O'Mathuna, N. Wang, S. Kulkarni, and S. Roy, "Review of integrated magnetics for power supply on chip (PwrSoC)," IEEE Transactions on Power Electronics, vol. 27, pp. 4799-4816, Nov. 2012

[2] G. Schrom, P. Hazucha, J. Hahn, D. S. Gardner, B. A. Bloechel, G. Dermer, et al., "A 480-MHz, multi-phase interleaved buck DC-DC converter with hysteretic control," 2004 IEEE 35th Annual Power Electronics Specialists Conference (PESC), 2004, pp. 4702-4707 Vol.6

[3] P. Zumel, C. Fernandez, A. de Castro, and O. Garcia, "Efficiency improvement in multiphase converter by changing dynamically the number of phases," in Proc. IEEE Power Electron. Spec. Conf., Jun. 2006, Jeju, South Korea, pp. 2845–2850

[4] E. Aklimi; D. Piedra; K. Tien; T. Palacios; K. L. Shepard, "Hybrid CMOS/GaN 40-MHz Maximum 20-V Input DC-DC Multiphase Buck Converter," in IEEE Journal of Solid-State Circuits , vol.PP, no.99, pp.1-10

[5] D. Hou; F. C. Lee; Q. Li, "Very High Frequency IVR for Small Portable Electronics with High-Current Multi-phase 3D Integrated Magnetics," in IEEE Transactions on Power Electronics , vol.PP, no.99, pp.1-1

[6] W. J. Lambert, M. J. Hill, K. Radhakrishnan, L. Wojewoda and A. E. Augustine, "Package Inductors for Intel Fully Integrated Voltage Regulators," in IEEE Transactions on Components, Packaging and Manufacturing Technology, vol. 6, no. 1, pp. 3-11, Jan. 2016

[7] N. Wang, T. O'Donnell, S. Roy, S. Kulkarni, P. McCloskey, and C. O'Mathuna, "Thin film microtransformer integrated on silicon for signal isolation," IEEE Transactions on Magnetics, vol. 43, pp. 2719-2721, Jun. 2007

[8] C. R. Sullivan, D. V. Harburg, Q. Jizheng, C. G. Levey, and Y. Di, "Integrating magnetics for on-chip power: A perspective," IEEE Transactions on Power Electronics, vol. 28, pp. 4342-4353, Sep. 2013

[9] N. Wang, R. Miftakhutdinov, S. Kulkarni, and C. O'Mathuna, "High efficiency on Si integrated micro-transformers for isolated power conversion applications," IEEE Transactions on Power Electronics, vol. 30, pp. 5746-5754, Oct. 2015

[10] Z. Pavlović, S. Kulkarni, N. Wang and C. Ó Mathúna, "High efficiency on-silicon coupled inductors using stacked copper windings," 2015 IEEE Energy Conversion Congress and Exposition (ECCE), Montreal, QC, 2015, pp. 5302-5307

[11] Y. Han, G. Cheung, A. Li, C. R. Sullivan and D. J. Perreault, "Evaluation of Magnetic Materials for Very High Frequency Power Applications," in *IEEE Transactions on Power Electronics*, vol. 27, no. 1, pp. 425-435, Jan. 2012

[12] M. Mu, Q. Li, D. J. Gilham, F. C. Lee and K. D. T. Ngo, "New Core Loss Measurement Method for High-Frequency Magnetic Materials," in IEEE Transactions on Power Electronics, vol. 29, no. 8, pp. 4374-4381, Aug. 2014

2168-6777 (c) 2018 IEEE. Personal use is permitted, but republication/redistribution requires IEEE permission. See http://www.ieee.org/publications_standards/publications/rights/index.html for more information.

This article has been accepted for publication in a future issue of this journal, but has not been fully edited. Content may change prior to final publication. Citation information: DOI 10.1109/JESTPE.2018.2798919, IEEE Journal of Emerging and Selected Topics in Power Electronics

[13] D. Hou, M. Mu, F. C. Lee and Q. Li, "New High-Frequency Core Loss Measurement Method With Partial Cancellation Concept," in IEEE Transactions on Power Electronics, vol. 32, no. 4, pp. 2987-2994, April 2017

[14] C. Fernandez, Z. Pavlovic, S. Kulkarni, P. McCloskey and C. O'Mathuna, "High Frequency, Single/Dual phases, Large AC/DC signal power characterization for two phase on-silicon coupled inductors", 2017 IEEE Applied Power Electronics Conference and Exposition (APEC), Tampa, FL, 2017

[15] Z. Pavlovic, C. Fernandez, S. Kulkarni, P. McCloskey and C. O'Mathuna, " High Frequency Large Signal Characterization for Two Phase on-silicon Coupled Inductors ", 2017 PwrSOC Workshopw on Integrated Power Conversion and Power Management, October 3-5 2016, Madrid, Spain

[16] S. Ziegler, R. C. Woodward, H. H. C. Iu and L. J. Borle, "Current Sensing Techniques: A Review," in IEEE Sensors Journal, vol. 9, no. 4, pp. 354-376, April 2009

[17] H. Li, S. Beczkowski, S. Munk-Nielsen, K. Lu and Q. Wu, "Current measurement method for characterization of fast switching power semiconductors with Silicon Steel Current Transformer," *2015 IEEE Applied Power Electronics Conference and Exposition (APEC)*, Charlotte, NC, 2015, pp. 2527-2531

[18] J. A. Ferreira, W. A. Cronje and W. A. Relihan, "Integration of high frequency current shunts in power electronic circuits," *Power Electronics Specialists Conference, 1992. PESC '92 Record., 23rd Annual IEEE*, Toledo, 1992, pp. 1284-1290 vol.2

[19] M. Danilovic, Z. Chen, R. Wang, F. Luo, D. Boroyevich and P. Mattavelli, "Evaluation of the switching characteristics of a gallium-nitride transistor," *2011 IEEE Energy Conversion Congress and Exposition*, Phoenix, AZ, 2011, pp. 2681-2688

[20] K. Li, A. Videt and N. Idir, "Using Current Surface Probe to Measure the Current of the Fast Power Semiconductors," in *IEEE Transactions on Power Electronics*, vol. 30, no. 6, pp. 2911-2917, June 2015

[21] G. Laimer and J. W. Kolar, "Accurate measurement of the switching losses of ultra-high switching speed CoolMOS power transistor/SiC diode combination employed in unity power factor PWM rectifier systems," in European Power Quality Conference (PCIM), Nuremberg (Germany), 2002, pp. 14-16

[22] S. Kulkarni, Z. Pavlovic, S. Kubendran, C. Carretero, N. Wang and C. O'Mathuna, "Large-signal power circuit characterization of on-silicon coupled inductors for high frequency integrated voltage regulation," 2016 IEEE Applied Power Electronics Conference and Exposition (APEC), Long Beach, CA, 2016, pp. 663-667

2168-6777 (c) 2018 IEEE. Personal use is permitted, but republication/redistribution requires IEEE permission. See http://www.ieee.org/publications_standards/publications/rights/index.html for more information.